Bull. Mater. Sci., Vol. 38, No. 5, September 2015, pp. 1277–1284. © Indian Academy of Sciences.

Synthesis and characterization of Sn-doped CdZnS nanoparticles

R SHRIVASTAVA[1,*] and S C SHRIVASTAVA[2]

[1]Department of Physics, Shri Shankaracharya Engineering College, Bhilai, Chhattisgarh 490 020, India
[2]Department of Mathematics, Rungta College of Engineering and Technology, Bhilai, Chhattisgarh 490 024, India

MS received 26 December 2014; accepted 16 April 2015

Abstract. Tin (Sn)-doped cadmium zinc sulphide nanoparticles (CdZnS : Sn) were synthesized by the chemical bath deposition method with two different concentrations of Sn (2 and 4 mol%). X-ray diffraction (XRD) pattern reveals the formation of CdZnS nanoparticles with cubic and hexagonal structure. It was observed that the presence of Sn does not alter the structure of CdZnS. Average crystallite size was measured from XRD data by using Scherrer's formula. From the study of absorption spectra, band-to-band absorption was obtained at 460 and 490 nm, respectively, for the Sn-doped (2 and 4 mol%) CdZnS nanoparticles. Energy bandgap for undoped and Sn-doped CdZnS varies from 3.5 to 2.9 eV with error ± 0.05 eV. The presence of Sn was confirmed by energy-dispersive X-ray analysis. The effect of dopant concentration on the photoluminescence (PL) intensity has also been studied. The PL emission peak has been observed at 540, 550 and 560 nm for the Sn-doped (CdZnS, CdZnS 2 mol% and CdZnS 4 mol%), respectively, nanoparticles. XRD and PL analyses demonstrate that the Sn^{2+} ions uniformly substitute Cd^{2+} sites or interstitial sites in CdZnS lattice, which influence the optical properties. Increase in the concentration of Sn shifts the UV–vis absorption spectra and PL emission spectra towards higher wavelength side. Particle size and the crystallinity of CdZnS : Sn nanoparticles were confirmed through atomic force microscopy.

Keywords. CdZnS; chemical bath deposition; thin films; structural properties.

1. Introduction

Cadmium zinc sulphide (CdZnS) alloy compounds have attracted technological interest, because the energy gap can be tuned and the lattice parameters can be varied.[1]

CdZnS films have been deposited in a variety of ways: vacuum evaporation, metalorganic chemical vapour deposition, chemical bath deposition (CBD), spray pyrolysis, successive ionic layer absorption and reaction (SILAR) and the dip technique. Among these techniques, CBD is most attractive because of its advantageous features over other deposition techniques and because it is a cheap and easily applicable technique. This method gives high-quality films at low temperatures, requires slow evaporation temperatures and easily coats very large surfaces. The only requirement for using this method is the knowledge of chemistry of the process.[2]

CdZnS thin films have been widely used as a wide bandgap window material in heterojunction solar cell[3–7] and in photoconductive devices.[8] In solar cell systems, where CdS films have been demonstrated to be useful, the replacement of CdS with the higher bandgap ternary CdZnS has led to a decrease in window absorption losses and has resulted in the increase of short-circuit current in the solar cell.[9] This CdZnS ternary compound is also potentially useful as a window material for the fabrication of p–n junctions without lattice mismatches of the devices based on quaternary materials like $CuIn_xGa_{1-x}Se_2$[10] or $CuIn(S_zSe_{1-z})_2$.[11] However, the resistivity of CdZnS films increases rapidly with the composition of zinc. It is evident that the composition dependence of resistivity is a basic property of the CdZnS solid-solution system and is not appreciably altered by the method of preparation. This high resistivity of CdZnS films limited their utilization as a doping material in most heterojunction devices. The resistivity can be reduced appreciably by an incorporation of donors and by doping the films with Sn. Earlier, Sn-doped CdS films, produced by using tartaric acid as complexing agent, were less transparent.[12] As the transmittance of light is the most important requirement of the window layer in a thin film structured solar cells, the search for methods to form very high transparent CdZnS films by doping Sn is highly warranted. In this paper, we present the fabrication of more transparent Sn-doped CdZnS films at a low dopant concentration by using the CBD technique. Additionally, the optical, structural and morphological properties of the films are also presented. The resulting CdZnS : Sn thin films were found to retain the beneficial optical properties for application as a window material in solar cells.

*Author for correspondence (ritu_10101010@rediffmail.com)

2. Experimental

In this study, nanocrystalline films were prepared on glass substrates by the CBD technique. The microscopic glass slides of dimensions 24 × 75 mm were used as substrates. The slides were first cleaned with H_2SO_4, acetone, double distilled water and ultrasonic cleaner. Then the dried glass slides were dipped vertically into a mixture of solution of 1 M cadmium acetate, 1 M zinc acetate, triethanolamine, 30% aqueous ammonia and thiourea. Briefly, 0.01 M $CdCl_2$ was used as flux and 0.01 M solution of $SnCl_2$ was used in varying concentrations. All solutions were prepared in double distilled water. The mixture was kept in a water bath for 1 h at 60°C temperature. The films were then formed on a glass substrate by doping the substrate in the mixture vertically. The prepared samples were then washed with double distilled water and dried at room temperature. The pH value of this mixture was found to vary from 11.2 at beginning to 10.9 pH at the end of the deposition.

3. Measuring instruments

X-ray diffraction (XRD) measurements in the incidence mode with 0.5° of beam inclination were performed, using a monochromatic CuKα radiation (λ = 1.540600 Å) and an aperture diaphragm of 0.2°, in a Rigaku RU : H2R X-ray diffractometer. Data were collected sequentially at a 2θ angle between 10° and 60°. An energy-dispersive X-ray analysis (EDAX) study was made by using a JEOL JSM 5600 scanning electron microscope (SEM). Transmission electron microscopy (TEM) measurements were made using a higher resolution electron microscope, Philips CM 120, operating at an accelerating voltage of 100 kV and capabilities of a point-to-point resolution of 2 Å. The photoluminescence (PL) excitation source was a high-pressure Hg source from which 365 nm radiation was selected by using Carl Zeiss interference filter. An RCA-6217 photomultiplier tube operated by a highly regulated power supply was used for the detection of PL light emission. The integrated light output in the form of current was recorded by a sensitive Polyflex galvanometer (10^{-9} A mm^{-1}). A prism monochromator was used for PL emission spectral studies. Optical absorption data were obtained with a Cary Bio 50 Varian UV–vis spectrophotometer.

4. Results and discussion

4.1 *XRD study*

XRD pattern of undoped CdZnS and Sn-doped CdZnS films are presented in figure 1. These patterns correspond to (100), (110), (111), (002), (211) and (220). These diffractographs show that the intensities of diffraction peaks

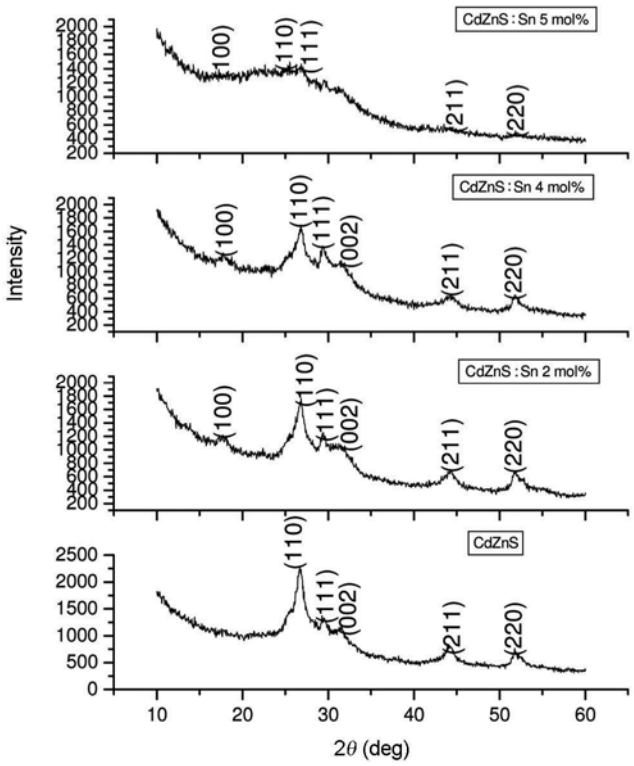

Figure 1. XRD spectra of CdZnS films with different doping concentrations of Sn and for undoped CdZnS.

declined as Sn concentrations increased, i.e., Sn doping within CdZnS films caused the crystallinity to degenerate. Moreover, the XRD pattern of CdZnS : Sn films that were prepared without the formation of secondary phase show high (002) peak intensities; which indicates that such film exhibits *c*-axis preferred orientation. In addition, increased Sn concentrations slightly shift the (110) peaks to higher diffraction angles. Sharma *et al*[13] have reported that the (110) peak shift to a high angle is because dopant ions have smaller radii than Cd^{2+} ions and dopant ions only substituted for Zn^{2+} ions. The average crystallite size (d) of these samples was estimated using Scherrer's formula[14]

$$L = \frac{0.94\lambda}{\beta\cos\theta},$$

where β is the full-width at half-maxima (FWHM) in radians, λ the X-ray wavelength of 1.5406 Å and θ the Bragg diffraction angle. The calculated average crystallite sizes of undoped CdZnS films were 15 nm. When the Sn concentration increases the average crystallite size decreases to about 1–2 nm.

4.2 *SEM study*

SEM micrographs of the film surfaces of CdZnS and CdZnS with 2 and 4 mol% Sn-doped films are shown in

Table 1. XRD results for CdZnS, CdZnS : Sn thin films for varying concentrations of Sn.

Sample	FWHM	2θ (deg)	d (nm)	(hkl)	Crystallite size	Lattice strain	I/I_0 (%)
CdZnS	1.198	26.6849	3.3375	110	7.12	0.0220	100
	0.6496	29.5823	3.017	111	13.21	0.0107	57
	0.4995	31.4806	2.389	002	17.27	0.0077	51
	0.3996	44.0692	2.053	211	22.41	0.0043	35.8
	0.7999	51.7622	1.264	220	11.53	0.0072	33.27
CdZnS : Sn 2 mol%	0.4995	17.693	5.0088	100	16.82	0.0140	69
	1.148	26.8348	3.31	110	7.43	0.0210	100
	0.5495	29.3325	3.04	111	15.62	0.0092	71
	0.4499	31.2308	2.86	002	19.16	0.0070	
	0.348	44.219	2.04	211	25.75	0.0037	40.2
	0.7492	51.7622	1.76	220	12.30	0.0067	37.27
CdZnS : Sn 4 mol%	0.6994	17.743	4.99	100	12.01	0.0196	75
	1.124	26.9347	3.31	110	7.59	0.0228	100
	0.4994	29.3325	3.04	111	17.18	0.0083	81.8
	0.399	30.1318	2.96	002	21.55	0.0065	69.61
	0.2996	44.1691	2.04	211	29.9	0.0032	37.87
	0.7493	51.8621	1.76	220	12.32	0.0067	38.46
CdZnS : Sn 5 mol%	0.1998	17.2434	5.137	100	22.02	0.0057	93.11
	0.996	25.5359	3.512	110	8.55	0.0192	97.25
	0.5197	29.4824	3.012	111	16.52	0.0086	100
	0.5495	43.5197	2.093	211	16.259	0.0060	40.86
	0.1998	51.8621	1.766	220	26.19	0.0018	34.44

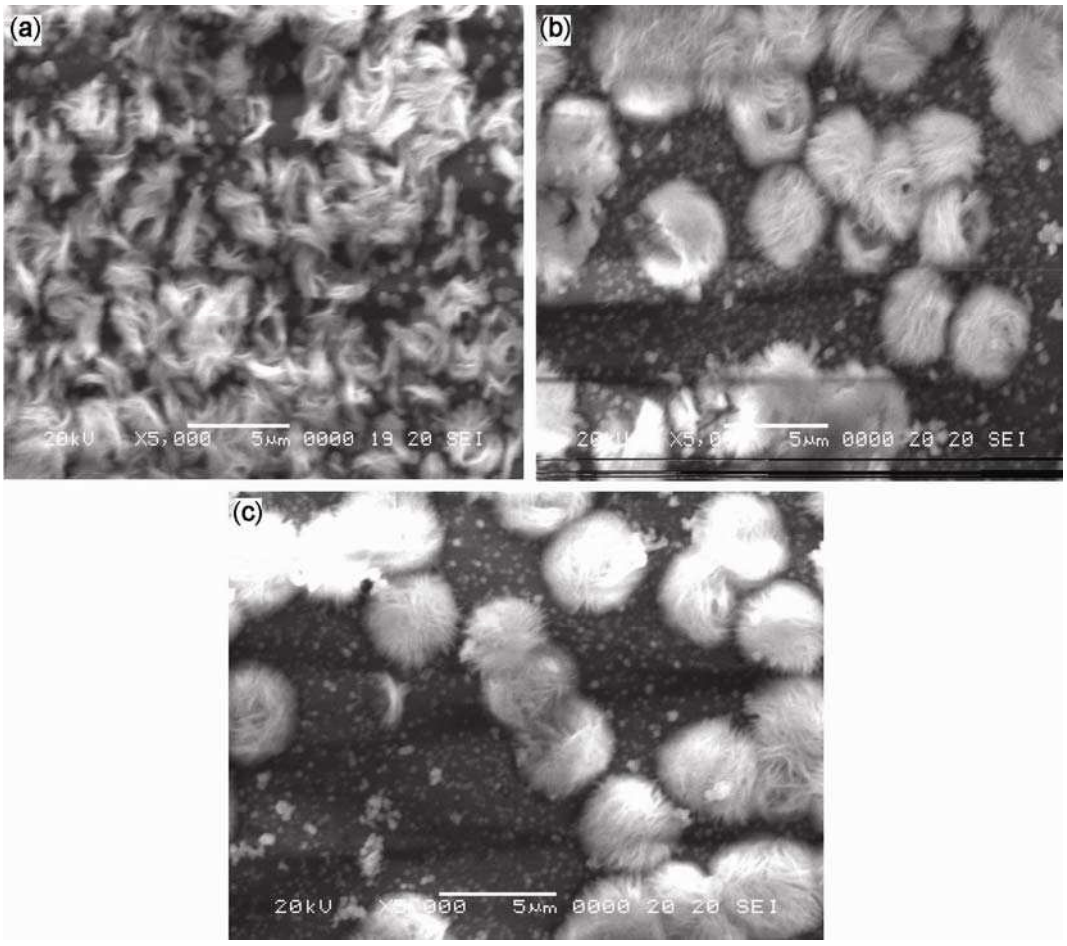

Figure 2. SEM micrograph of (**a**) undoped CdZnS, (**b**) 2 mol% Sn-doped CdZnS and (**c**) 4 mol% Sn-doped CdZnS films.

figure 2a–c, respectively. These images reveal that the films are compact, free of colloidal particles and are in good order. The plane view of SEM micrographs of undoped CdZnS films shows the leafy-like structure. However, the doped samples do not display the appearance from the surface micrographs of 2, 4 and 5 mol% $SnCl_2$-doped CdZnS films. According to the previous report[15] the leafy-like or fiber-like structure was induced by the shortness of OH and OR groups. Thus, a relatively smooth surface will be obtained when component materials can provide enough OH and OR groups. The sizes of grains were in the same range as those that show homogeneous distribution of Sn dopant in films. Increasing the dopant led to grain growth. The surface grain size becomes larger with less void area, and led to the formation of high-quality film surfaces. These SEM micrographs also reveal that Sn doping of CdZnS films can increase the average crystallite size. The grain size for undoped, 2 and 4 mol% doped films are 4.748, 5.929 and 8.525 nm, respectively (as determined by IMAGE J software). The result agrees with XRD measurements.

4.3 *AFM study*

AFM images of the CdZnS : Sn thin films are shown in figure 3a–c. These images show that the surface morphologies of the films were strongly dependent on the dopant concentration. In addition, it is apparent that the reduction of surface roughness results from an increase in the average crystallite size in the CdZnS films after Sn substitution. The plot of surface levels of CdZnS : Sn thin films as a function of Sn concentration is shown. A significant improvement of surface roughness with Sn doping can be noticed. The RMS value decreases with the increase in Sn.

We calculated another two parameters, i.e., the skewness (S_{sk}) parameter and the kurtosis parameter (S_{ku}).[16] Both the parameters have no units, they are pure numbers

$$S_{sk} = \frac{1}{MNS_q^3} \sum_{k=0}^{M-1} \sum_{l=0}^{N-1} [z(x_k, y_l) - \mu]^3,$$

$$S_{ku} = \frac{1}{MNS_q^4} \sum_{k=0}^{M-1} \sum_{l=0}^{N-1} [z(x_k, y_l) - \mu]^4.$$

The S_{sk} parameter has been used in order to describe the asymmetry of the height distribution histogram. It was seen that the S_{sk} parameter exhibit a positive value close to zero. This indicates a symmetric height distribution. Another descriptive parameter is the kurtosis one: smaller values of the S_{ku} parameter indicate broader height

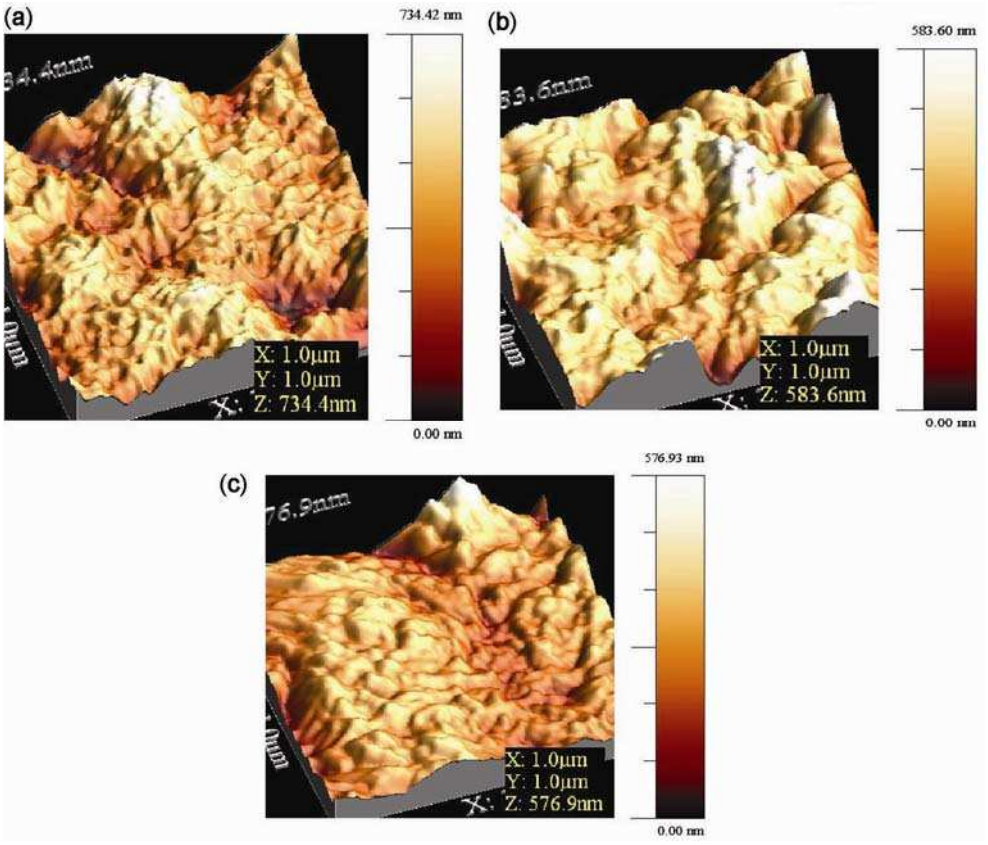

Figure 3. AFM micrograph of (**a**) CdZnS, (**b**) CdZnS : Sn 2 mol% and (**c**) CdZnS : Sn 4 mol% thin films.

Table 2. Roughness profiles of CdZnS and CdZnS : Sn thin films with varying concentrations of Sn.

Film	RMS value	Roughness average	Skewness	Kurtosis
CdZnS	104	81.9213	0.0761	3.258
CdZnS : Sn 2 mol%	79	62.97	0.0787	3.2414
CdZnS : Sn 4 mol%	61	48	0.127	4.0318

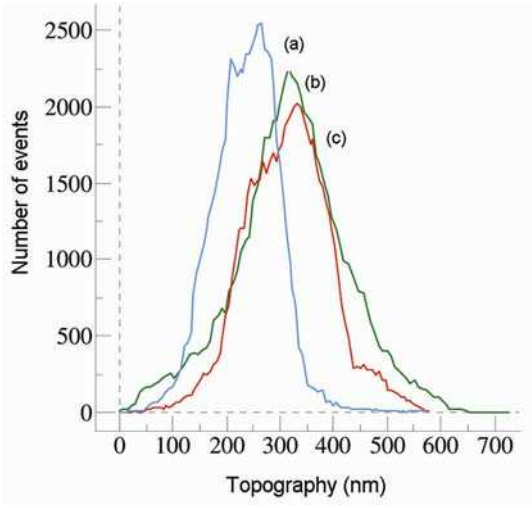

Figure 4. Roughness profiles of (**a**) CdZnS, (**b**) CdZnS : Sn 2 mol% and (**c**) CdZnS : Sn 4 mol% films for undoped and Sn-doped film.

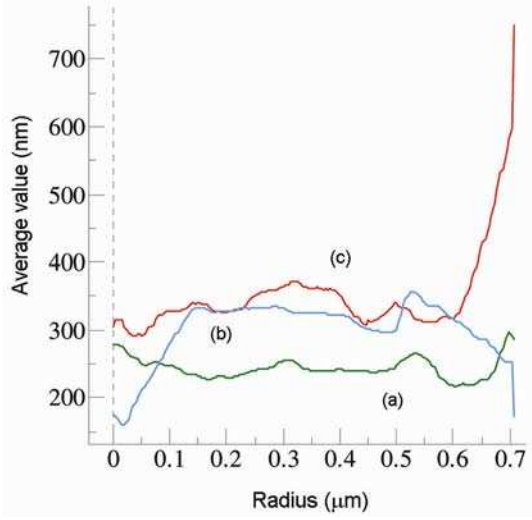

Figure 5. Average radial profile for (**a**) CdZnS, (**b**) CdZnS : Sn 2 mol% and (**c**) CdZnS : Sn 4 mol% films.

distribution, whereas values higher than 3.0 indicate sharper height distribution.[16] At the microscale (hundreds of microns) the employed surface is relatively smooth and uniform. At the nanoscale, all the samples showed small irregularities, which can be seen in AFM images. The rough surfaces of the component attributed to the small grain size. This is also clear from table 2.[3] Also the typical average roughness profile for respective samples is shown in figure 4. This can determine the growth and coalescence of randomly oriented grains of different sizes. The average radial profile is shown in figure 5. It is clear that the average radial value increases with the increase in the doping concentration of Sn. It is also in a good agreement with XRD and SEM results.

4.4 *EDAX study*

EDAX spectrum, as shown in figures 6–8, of CdZnS, CdZnS : Sn 2 mol% and CdZnS : Sn 4 mol% nanoparticles, respectively, shows the presence of major chemical elements, namely cadmium, sulphur, zinc and Sn. An intense peak for Sn was found in the spectrum due to its higher concentration as in comparison to cadmium and zinc. The elemental composition analysis for Sn-doped CdZnS is shown in the table 3, which also confirms that majority of Sn^{2+} ions are doped with CdZnS. The traces of Si and O are due to the glass substrate.

4.5 *PL studies*

Upon excitation at 350 nm, the samples show luminescence in the blue region. As the Sn concentration increases the intensity of luminescence increases effectively. The intensity of 0.01 M Sn-doped samples is enhanced to that of the undoped sample. The enhancement in the emission intensity on Sn doping is attributed to the increase of defect densities in the bandgap. The emission peak for Sn-doped CdZnS sample shifted to red region with increasing intensity in the spectrum as compared to the base material CdZnS. Thus, it confirms that luminescence property of nanoparticles enhanced when Sn was introduced into the lattice.[17] Similar explanation was given by Devi *et al*[18] for the peak nanocrystalline CdS.

The PL spectra of the nanocrystalline CdZnS samples are shown in figure 9. A peak was obtained at 540, 550 and 560 nm for CdZnS, CdZnS : Sn 2 mol% and 4 mol% samples corresponding to bandgap 3.5 ± 0.05, 3.0 ± 0.05 and 2.9 ± 0.05 eV, respectively. It can be noted that the PL peak is obtained at photon energies less than the effective peak observed by absorption peak, and the peak shifts towards higher wavelength with increasing particle size. When the particle size increases, the effective bandgap decreases, therefore the emitted photon has a comparatively higher wavelength peak, which may be

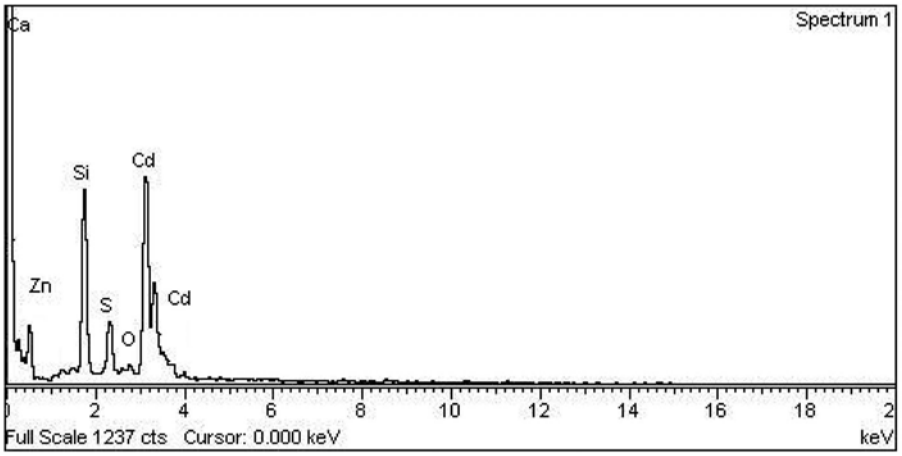

Figure 6. EDAX spectra of undoped CdZnS films.

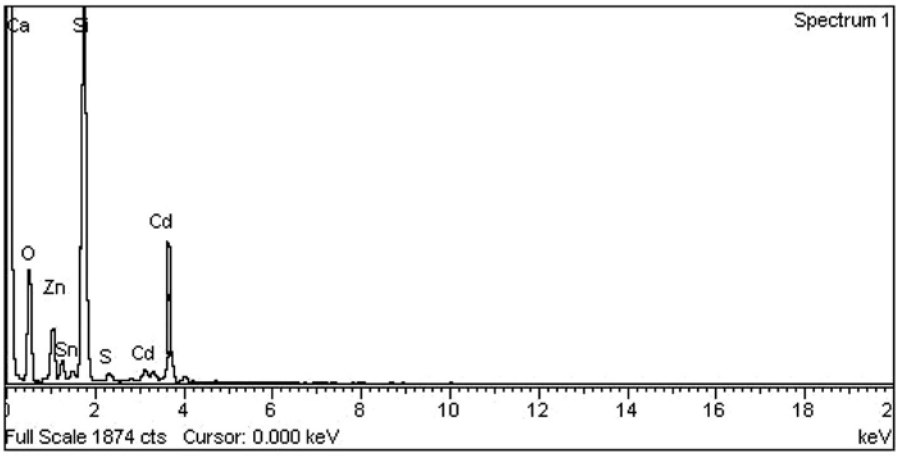

Figure 7. EDAX spectra for CdZnS : Sn film with 2 mol% Sn.

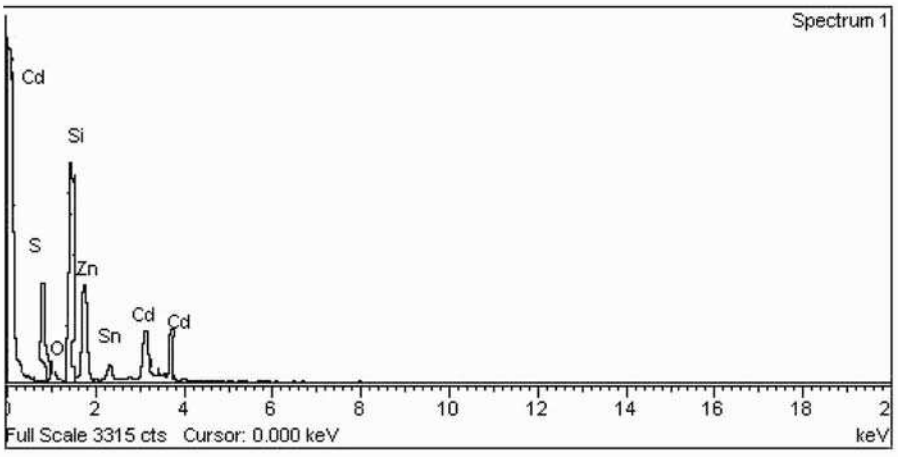

Figure 8. EDAX spectra for CdZnS : Sn film doped with 4 mol% Sn.

due to the edge emission of CdZnS. Thomos and Hopfield[19,20] attributed the edge emission to transitions associated with donor/acceptor exciton complexes. Jeong and Yu[20] observed the excitonic effects in CdS at RT. Thus, in the present case also the edge emission can be attributed to excitonic transitions. In the present study, a single broad peak is observed in CdZbS : Sn. Due to the similar excitonic nature of emission it can be attributed to

Table 3. EDAX elemental analysis for undoped CdZnS and CdZnS : Sn for 2 and 4 mol% Sn doping.

	CdZnS		CdZnS : Sn 2 mol%		CdZnS : Sn 4 mol%	
Elements	Weight (%)	Atomic (%)	Weight (%)	Atomic (%)	Weight (%)	Atomic (%)
Cd	53.27	10.71	77.54	64.99	50.69	63.12
Zn	5.43	5.34	6.62	2.22	6.97	6.04
S	46.25	65.31	48.84	23.32	37.77	6.69
Si	17.13	13.77	11.36	6.62	26.37	18.71
O	4.89	3.44	6.65	0.87	3.56	1.77
Sn	–	–	2.63	1.45	3.90	2.42
Ca	2.52	1.42	1.27	0.53	1.52	1.25

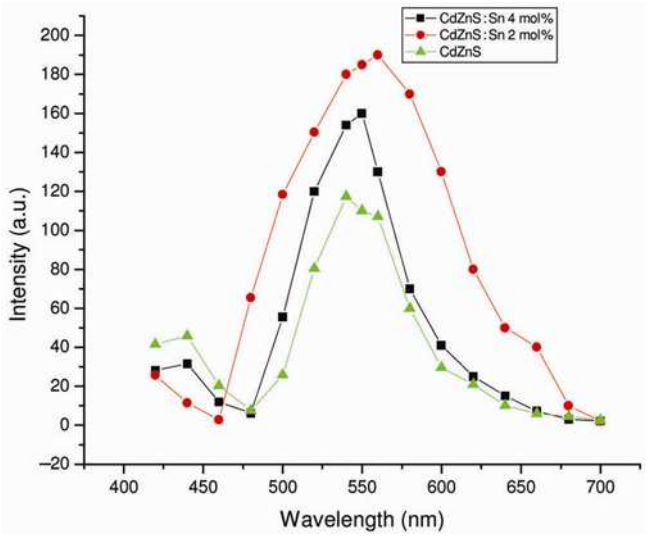

Figure 9. PL emission spectra of CdZnS and CdZnS : Sn with 2 and 4 mol% Sn doping.

radioactive decay of free exciton. The PL emission in CdZnS : Sn is significantly broader than pure CdZnS due to excitonic effects.[2,19] Full-width at half-maxima (FWHM) of the CdZnS is reduced with the Sn doping into CdZnS, the reduction in the FWHM of the green emission peak is possibly due to the formation of new recombination centres with Sn doping. Compared with the undoped CdZnS, the PL spectra of the doped CdZnS nanostructures show a red shift in the emission spectra. This shift may be attributed to the shrinkage of bandgap and also the increasing carrier concentration with Sn doping.

4.6 *UV absorption spectra*

The absorption spectra of undoped CdZnS and Sn-doped CdZnS films were measured in the range of 200–800 nm; based on the absorption spectra the optical bandgap E_g was obtained by extrapolating the linear portion of the plot $(\alpha h\nu)^2$ *vs.* $h\nu$ to $\alpha = 0$ according to the following equation

$$\alpha = A(h\nu - E_g)^n,$$

where $h\nu$ is the photon energy, E_g the optical bandgap, A the edge parameter and $n = 1/2$ for direct gap material.

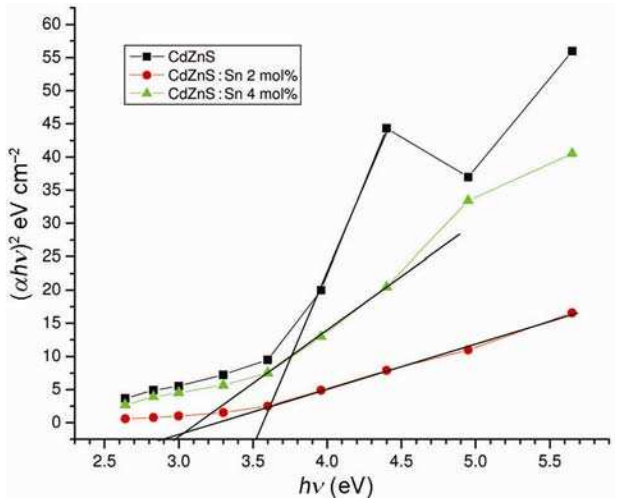

Figure 10. Tauc's plot for CdZnS and CdZnS : Sn film with 2 and 4 mol% Sn doping.

The optical bandgap E_g of undoped CdZnS and Sn-doped CdZnS films is shown in figure 10. UV-absorption spectra of the CdZnS nanoparticles for pure 2 and 4 mol% Sn doping are shown in figure. Based on these absorption spectra the absorption edge for each compound was determined. Optical studies show that the bandgap decreases significantly for pure CdZnS to Sn-doped CdZnS.[21,22] Band-to-band absorption is seen at 3.5 ± 0.05, 3 ± 0.05 and 2.9 ± 0.05 eV, respectively, for pure CdZnS and CdZnS : Sn for 2, 4 mol% Sn-doped nanoparticles. Increase in Sn doping concentration decreases the optical bandgap of CdZnS films. This shift in the optical bandgap may be attributed to the band shrinkage effect because of increasing carrier concentration.[23] Decrease in the bandgap for Sn doping can also be explained on the basis of the model of density of states in amorphous solids proposed by Mott and Davis.[24] The small shift in the absorption peaks is attributed to the doping of Sn into CdZnS. With doping of Sn absorption edge slightly shifts towards the longer wavelength region, which may be attributed to the increase in the grain size.

5. Conclusions

CdZnS : Sn nanoparticles with different Sn concentrations have been synthesized by the chemical bath deposition

method. XRD pattern reveals the formation of cubic and hexagonal structures of CdZnS : Sn (2 and 4 mol%) with peak shift towards lower angle, which confirms the incorporation of Sn. XRD studies show that crystallite size increases with the increase in the concentration of Sn. EDAX spectra support the presence of major chemical element. SEM study shows that grain size increases with the increase in the concentration of Sn. AFM study indicates that roughness of film surface decreases, whereas average radial value increases with the increase in the concentration of Sn. Compared to pure CdZnS, the decrease in the band-gap energy value of CdZnS : Sn nanoparticles illustrates quantum confinement effect. For Sn-doped CdZnS, the emission intensity was found to be a maximum with slight shift towards the higher wavelength compared to bulk CdZnS. Intense PL emission was observed for the incorporation of Sn ions into CdZnS nanoparticles, which will be useful for high-efficient EL devices and also possible for making full colour device applications.

Acknowledgements

We thank Dr V Ganesan, Dr Mukul Gupta, Dr N P Lalla and Dr Phase UGC-DAE-CSR, Indore, for providing XRD, AFM, TEM and SEM with EDAX facilities. We are also thankful to Mr Mohan Kumar Gangrade, Mr Layanta Behra and Ms Preeti Bhardwaj for conducting the measurements.

References

1. Maqbool M, Ahmad I, Richardson H H and Kordesch M E 2007 *Appl. Phys. Lett.* **91** 193511
2. Karpier I A 2014 *Int. J. Miner. Metall. Mater.* **21** 832
3. Maqbool M, Richardson H H and Kordesch M E 2007 *J. Mater. Sci.* **42** 5657
4. Maqbool M 2006 *Eur. Phys. J. Appl. Phys.* **34** 31
5. Okamoto K, Yoshimi T and Miura S 1988 *Appl. Phys. Lett.* **53** 678
6. Jayaraj M K and Vallabhan C P G 1991 *J. Electrochem. Soc.* **138** 1512
7. Lozykowski H J, Jadwisienkzak W M and Brown I 2000 *J. Appl. Phys.* **88** 210
8. Liu G K, Zhuang H Z and Chen X Y 2002 *Nano Lett.* **2** 535
9. Zych E, Hreniak D and Strek W 2002 *J. Phys. Chem. B* **106** 3805
10. Liqiang J, Xiaojun S, Baifu X, Baiqi W, Weimin C and Honggang F 2004 *Mater. Sci. Technol.* **12** 148
11. Guo G, Li D, Wang Z and Guo H 2005 *J. Rare Earths* **23** 362
12. Vij A, Singh S, Kumar R, Lochab S P, Kumar V V S and Singh N 2009 *J. Phys. D: Appl. Phys.* **42** 105103
13. Sharma G, Chawla P, Lochab S P and Singh N 2009 *Radiat. Effects Defects Solids* **164** 763
14. Kumar V, Pitale S S, Mishra V, Nagpure I M, Biggs M M and Ntwaeaborwa O M 2010 *J. Alloys Compd.* **492** L8-5
15. Petre D, Pintilie I, Pentia E, Pintilie I and Botila T 1999 *Mater. Sci. Eng. B* **58** 238
16. Khallaf H, Chai G, Lupan O, Chow L, Park S and Schulte A 2009 *Appl. Surf. Sci.* **255** 4129
17. Davila-Pintle J A, Lozada-Morales R L, Palomino-Merino M R, Rivera-Márquez J A, Portillo-Moreno O P and Zelaya-Angel O Z 2007 *J. Appl. Phys.* **101** 013712
18. Devi R, Kalita P K, Purkayastha P and Sharma B K 2008 *Indian J. Phys.* **82** 707
19. Thomas D G and Hopfield J 1962 *J. Phys. Rev.* **128** 2135
20. Jeong T S and Yu P Y 2000 *J. Phys. Soc. (Korea)* **36** 102
21. Roy P and Srivastava S K 2009 *J. Phys. D* **39** 4771
22. Saravanan L 2012 *Mater. Lett.* **66** 343
23. Benelmadjat H, Boudine B, Halimi O and Sebais M 2009 *Opt. Laser Technol.* **41** 630
24. Mott N and Davis E 1979 *Electronic processes in non-crystralline materials* (Oxford, UK: Clarendon) 2nd edn, vol. 17, p 122